

Relation between the electroforming voltage in alkali halide-polymer diodes and the bandgap of the alkali halide

Benjamin F. Bory, Jingxin Wang, Henrique L. Gomes, René A. J. Janssen, Dago M. De Leeuw, and Stefan C. J. Meskers

Citation: *Applied Physics Letters* **105**, 233502 (2014); doi: 10.1063/1.4903831

View online: <http://dx.doi.org/10.1063/1.4903831>

View Table of Contents: <http://scitation.aip.org/content/aip/journal/apl/105/23?ver=pdfcov>

Published by the [AIP Publishing](#)

Articles you may be interested in


[Electronic structure, lattice energies and Born exponents for alkali halides from first principles](#)
AIP Advances **2**, 012131 (2012); 10.1063/1.3684608

[Thermal diffusivity of alkali and silver halide crystals as a function of temperature](#)
J. Appl. Phys. **109**, 033516 (2011); 10.1063/1.3544444





[Thermal conductivity of molten alkali halides: Temperature and density dependence](#)
J. Chem. Phys. **130**, 044505 (2009); 10.1063/1.3064588

[Cationic effects in polymer light-emitting electrochemical cells](#)
Appl. Phys. Lett. **89**, 253514 (2006); 10.1063/1.2422877

[Electronic line-up in light-emitting diodes with alkali-halide/metal cathodes](#)
J. Appl. Phys. **93**, 6159 (2003); 10.1063/1.1562739



Instruments for Advanced Science

 <p>Gas Analysis</p> <ul style="list-style-type: none">dynamic measurement of reaction gas streamscatalysis and thermal analysismolecular beam studiesdissolved species probesfermentation, environmental and ecological studies	 <p>Surface Science</p> <ul style="list-style-type: none">UHV TPDSIMSend point detection in ion beam etchelemental imaging - surface mapping	 <p>Plasma Diagnostics</p> <ul style="list-style-type: none">plasma source characterizationetch and deposition process reactionkinetic studiesanalysis of neutral and radical species	 <p>Vacuum Analysis</p> <ul style="list-style-type: none">partial pressure measurement and control of process gasesreactive sputter process controlvacuum diagnosticsvacuum coating process monitoring
--	---	---	---

Contact Hiden Analytical for further details:
W www.HidenAnalytical.com
E info@hiden.co.uk
CLICK TO VIEW our product catalogue

Relation between the electroforming voltage in alkali halide-polymer diodes and the bandgap of the alkali halide

Benjamin F. Bory,¹ Jingxin Wang,¹ Henrique L. Gomes,² René A. J. Janssen,¹ Dago M. De Leeuw,³ and Stefan C. J. Meskers^{1,a)}

¹Molecular Materials and Nanosystems and Institute for Complex Molecular Systems, Eindhoven University of Technology, P.O. Box 513, 5600 MB Eindhoven, The Netherlands

²Instituto de Telecomunicações, Av. Rovisco, Pais 1, 1049-001 Lisboa, Portugal and Universidade do Algarve, Campus de Gambelas, 8005-139 Faro, Portugal

³Max-Planck Institute for Polymer Research, Ackermannweg 10, 55128 Mainz, Germany and King Abdulaziz University, Jeddah, Saudi Arabia

(Received 16 September 2014; accepted 28 November 2014; published online 9 December 2014)

Electroforming of indium-tin-oxide/alkali halide/poly(spirofluorene)/Ba/Al diodes has been investigated by bias dependent reflectivity measurements. The threshold voltages for electrocoloration and electroforming are independent of layer thickness and correlate with the bandgap of the alkali halide. We argue that the origin is voltage induced defect formation. Frenkel defect pairs are formed by electron-hole recombination in the alkali halide. This self-accelerating process mitigates injection barriers. The dynamic junction formation is compared to that of a light emitting electrochemical cell. A critical defect density for electroforming is $10^{25}/\text{m}^3$. The electroformed alkali halide layer can be considered as a highly doped semiconductor with metallic transport characteristics. © 2014 Author(s). All article content, except where otherwise noted, is licensed under a Creative Commons Attribution 3.0 Unported License.

[<http://dx.doi.org/10.1063/1.4903831>]

The electrical resistance of metal-insulator-metal diodes with wide-bandgap ionic semiconductors can be switched after electroforming upon applying a high bias voltage. The change in resistance is often non-volatile and can be utilized in electronic storage of information.¹ In the operation of such resistive switching electronic memory cells, the ability to control the electroforming step is the key to the success as a device technology. Electroforming has been investigated especially for metal oxides.^{2–5} The forming process is due to ‘soft’ dielectric breakdown of the oxide,⁶ and has been related to formation of oxygen vacancies in the oxide.⁷ However, apart from metal oxides, also metal halides show electroforming and resistive switching^{8,9} and provide another model system to elucidate mechanism(s) of electroforming.

Here, we investigate electroforming in metal-alkali halide-semiconducting polymer-metal diodes. The semiconducting polymer acts as a current limiter preventing ‘hard’ breakdown, resulting in fully shorted diodes.¹⁰ The alkali halides provide a homologous series of wide-bandgap ionic semiconductors. We find that the bias voltage required for electroforming of alkali halide-polymer diodes correlates with the bandgap of the alkali halide and involves electrocoloration of the semiconductor. The electro-optical data are consistent with defect formation in alkali halides^{11,12} with electrogenerated (self-trapped) excitons as intermediate, i.e., the same mechanism as for creation of radiation induced defects. Voltage-induced defect formation is a self-accelerating process in which defects formed mitigate injection barriers for parental charge carriers. As a consequence,

the electroforming voltage is reduced to the bandgap of the ionic semiconductor.

Indium-tin-oxide(ITO)/alkali halide/poly(spirofluorene)/Ba/Al diodes were fabricated by thermal sublimation of alkali halide under 10^{-6} millibar onto glass substrates with patterned ITO. ITO substrates were cleaned, using in order, acetone, soap scrubbing, and isopropanol. The poly(spirofluorene) (Merck, SPB-02T) was dissolved in toluene at a concentration of 10 mg/ml and spin coated at a speed of 3500 rpm. Subsequently, Ba and Al were deposited by sublimation under vacuum. Diodes on ITO substrates were kept under inert atmosphere (N_2 ; O_2 , $\text{H}_2\text{O} < 1$ ppm) at all times during fabrication and characterization. Throughout this study, positive bias is defined as the ITO bottom electrode being charged positive. Current density-voltage (J - V) characteristics were recorded with an Agilent 4155C semiconductor parameter analyzer. J - V sweeps were recorded with 50 mV step and 40 ms integration time. Reflection experiments were performed using a Perkin Elmer Lambda 900 UV-Vis-NIR spectrometer with a module for specular reflection measurements.

To induce electroforming, pristine ITO/alkali halide/poly(spirofluorene)/Ba/Al diodes were submitted to sequential cyclic current-voltage (J - V) scans with stepwise increase of the maximum bias, see Fig. 1. The current densities show a specific type of hysteresis. In the forward scan at a voltage to which the diode has not been subjected before, the current density is considerable and depends on the sweep rate. In the backward part of the scan, the current density is much smaller. Furthermore, current densities at voltages that have already been applied to diode before, are much lower. This peculiar, history dependent hysteresis in the J - V characteristics has been reported for metal/ Al_2O_3 /poly(spirofluorene)/metal diodes and is attributed to trapping of electrons.¹³

^{a)}Author to whom correspondence should be addressed. Electronic mail: s.c.j.meskers@tue.nl

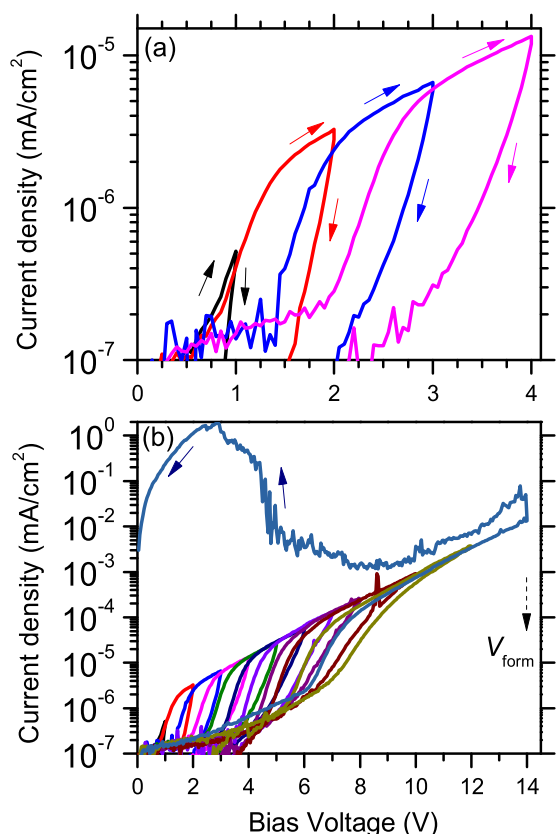


FIG. 1. J - V characteristics of a pristine ITO/LiF (80 nm)/poly(spirofluorene)(80 nm)/Ba/Al diode during subsequent cyclic voltage sweeps ($0\text{ V} \rightarrow V_{\text{max}} \rightarrow 0\text{ V}$) where the maximum voltage V_{max} is raised in steps of 1 V. (a) the initial scans up to $V_{\text{max}} = +4\text{ V}$. (b) The complete series of sweeps ending with electroforming at $V_{\text{form}} = +14\text{ V}$.

When the bias applied to the ITO/LiF/poly(spirofluorene)/Ba/Al reaches 14 V, a sudden increase in current density occurs (Fig. 1). Upon the backward sweep from +14 V to zero bias, the current density remains high. Near zero bias, the J - V characteristic is almost Ohmic. The diode has become electroformed. We mark the voltage at which the surge in current density occurs (+14 V) as the electroforming voltage.

Forming voltages for diodes with alkali halide layers of different thickness were determined.^{14,15} We find no significant variation with the thickness of the alkali halide, which shows that the electroforming process is not driven by the electric field. The electroforming has been investigated for a series of alkali halides. In Fig. 2(a), electroforming voltages for ITO/alkali halide/poly(spirofluorene)/Ba/Al diodes with 10 different alkali halides are shown as function of the electronic bandgap of the alkali halide.¹⁶ As can be seen, the forming voltage correlates with the bandgap of the alkali halide.

To further investigate electroforming, we have employed optical reflection spectroscopy as a function of applied bias. The use of a transparent ITO bottom contact allows optical access to the semiconducting alkali halide and polymer layers. The metal back electrode acts as a mirror. As an example, we show in Fig. 3 the influence of continuously applied bias voltage on the reflection of light by ITO/CsI(100 nm)/poly(spirofluorene)/Ba/Al diode. Application of bias voltage up to +2 V does not result in any significant changes in reflectance.

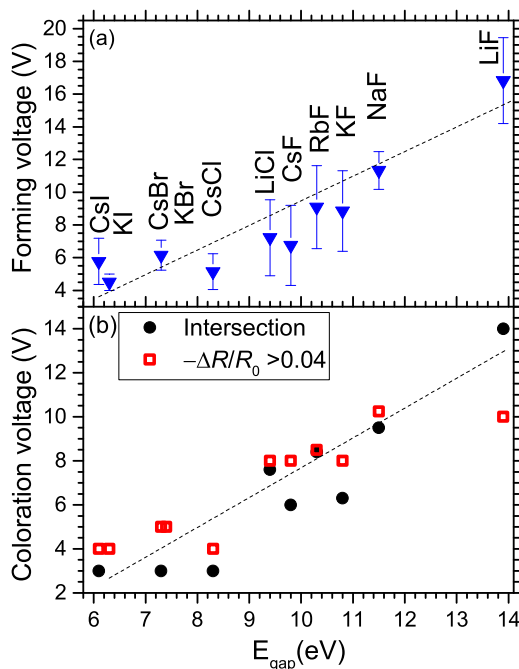


FIG. 2. (a) Electroforming voltages for ITO/alkali halide/poly(spirofluorene)(80 nm)/Ba/Al diodes plotted versus the band gap of the alkali halide. Error bars indicate the standard deviation of the set of measurements. (b) Electrocoloration voltage ITO/alkali halide/poly(spirofluorene)(80 nm)/Ba/Al diodes. The thickness of the alkali halide layers is 100 nm, except for LiCl where it is 50 nm. Dashed lines serve as a guide to the eye.

However, bias voltages exceeding +2 V induce a change in reflectance $\Delta R = R(x\text{ volt}) - R(0\text{ volt})$. The relative change in reflectivity $-\Delta R/R_0$ with R_0 the reflectance at zero bias shows a broad absorption band at 1.03 eV photon energy. We attribute this band to voltage induced defects in the alkali halide layer. The bias voltage at which the relative change in reflectance $\Delta R/R_0$ exceeds 0.04 is arbitrarily taken as the electrocoloration voltage (V_{color}).

The voltage-induced changes in the reflectivity of the diodes are fully reversible for bias voltages below the electroforming voltage. In Fig. 4, we illustrate the time evolution of the normalized reflectance of a ITO/CsI(100 nm)/poly(spirofluorene)(80 nm)/Ba/Al diode probed at 1.0 eV photon

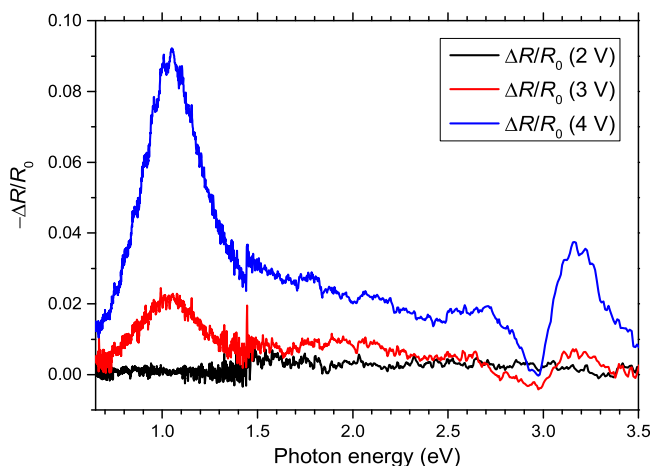


FIG. 3. Relative differential reflectance $-\Delta R/R_0$ versus photon energy for an ITO/CsI(100 nm)/poly(spirofluorene)(80 nm)/Ba/Al diode for different values of the applied bias voltage. R_0 is the reflectivity of the pristine diode.

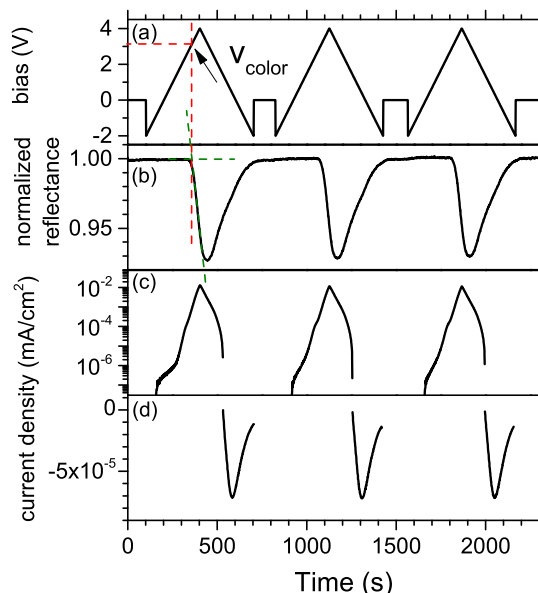


FIG. 4. Normalized reflectance R and current density J for an ITO/CsI (100 nm)/poly(spirofluorene) (80 nm)/Ba/Al diode as function of time during application of the time-dependent bias voltage shown in (a). The dashed lines show the graphical determination of the electrocoloration voltage V_{color} . (b) Normalized reflectance at a photon energy of 1.0 eV. (c) Positive part of the current density J . (d) negative part of the current density.

energy, during the application of a time-dependent bias voltage with saw tooth profile (see Fig. 4(a)). The profile includes intervals of zero bias to ensure equilibration of the diode. While ramping the bias from -2 to $+4$ V (see Fig. 4(b)), a sudden drop in the reflectivity occurs when the bias voltage exceeds $+3$ V. Upon reaching the maximal bias, the reflectance reaches a minimum and fully recovers when lowering the bias again to 0 volt. The electrocoloration can be repeated several times.

The onset voltage for electrocoloration can be determined as shown in Fig. 4(a) by extrapolating the baseline and the linear part of the downward sloping reflectance-time curve. The voltage at which the two extrapolated lines intersect is an alternative measure for V_{color} . For CsI, we then find a coloration voltage $V_{color} = +3$ V, practically independent of the thickness of the CsI layer.¹⁴ Coloration voltages for all alkali halides investigated, determined by the two methods discussed above, are shown in Fig. 2(b). The coloration voltage, which is generally lower than the electroforming voltage, also correlates with the bandgap of the alkali halide.

The current densities through the ITO/CsI/polyspirofluorene diodes have been measured simultaneously with the bias voltage dependence of the optical reflectivity, see Figs. 4(c) and 4(d). When increasing the bias from -2 to $+4$ V, the current density approaches an exponential dependence on bias. Upon lowering the bias from $+4$ V, the current density becomes negative at $+1$ V bias and reaches its most negative value around zero bias. Upon further decreasing the bias to -2 V, the current density decays to zero. The negative, transient current under short-circuit conditions indicates the release of charge accumulated in the semiconducting layers under forward bias. Integrating this negative part of the current density, we find that approximately 4×10^{17} elementary charges can be stored in the diode per m^2 . This

number is essentially independent of the thickness of the CsI layer, and similar densities are obtained for other alkali halides.¹⁴ The charge density extracted is more than an order of magnitude larger than estimated for a capacitor with a 100 nm thick, fully insulating alkali halide layer with $\epsilon_r = 9$. Hence, we argue that upon application of a bias, positive charge is accumulated in the alkali halide layer.

In the next paragraphs, we present a step-by-step interpretation of the experimental data presented above in terms of a tentative, comprehensive model for electrocoloration and electroforming that is illustrated graphically in Fig. 5. When applying positive bias voltage to the ITO/alkali halide/poly(spirofluorene)/Ba/Al diodes, electrons are injected into the polymeric semiconductor via the quasi-Ohmic Ba/Al electrode¹⁷ and get trapped in deep trap sites at the alkali halide/polymer interface (See Fig. 5(a)). The trapping of electrons explains the hysteresis in the low voltage range illustrated in Fig. 1.^{13,14} The nature of these trap sites is not known; ubiquitous water and molecular oxygen are likely candidates.

At higher bias, but still lower than the bandgap, the alkali halide starts to conduct electrons (Fig. 5(b)). We note that in this bias region, the diodes show high rectification, which excludes leakage currents via shorts.^{14,15} The electron current is supported by the high mobility of electrons in alkali halides¹⁸ and detailed analysis of the voltage dependence for diodes containing LiF layers of different thickness.¹⁹ The trapping of electrons induces alignment of the conduction bands of polymer and alkali halide and facilitates the transport of electrons through the alkali halide. The presence of electrons in the alkali halide is a prerequisite for electron-hole recombination leading to defect formation (see below).

Importantly, when the bias voltage exceeds the bandgap of the alkali halide ($V \geq E_g$, Fig. 5(c)), injection of holes becomes energetically allowed. There still is a large injection barrier for this minority carrier; hence, the rate for hole

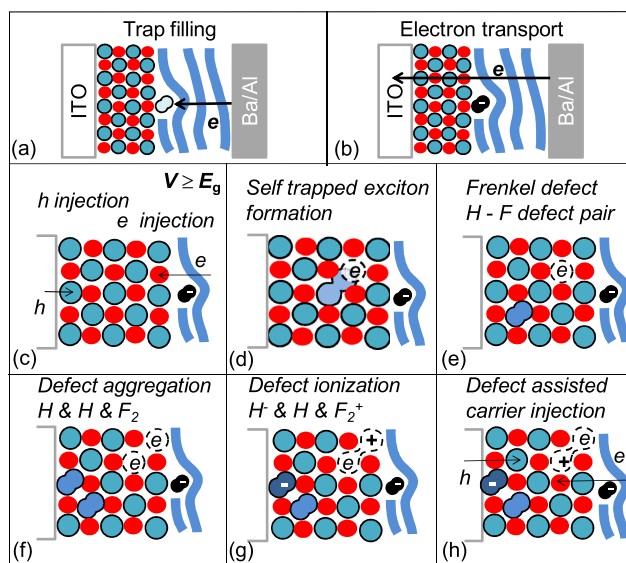


FIG. 5. Schematic representation of elementary processes leading to electrocoloration and eventually electroforming of ITO/alkali halide/poly(spirofluorene)/Ba/Al diodes. Blue ribbons represent chains of poly(spirofluorene), red and blue dots the alkali and halide ions. Panels (a)–(h) correspond to subsequent processes induced by increasing bias voltage.

injection is initially low. However, as we will argue below, injection of a hole with small but finite probability starts a self-accelerating process resulting in a lowering of the injection barrier. Electroluminescence measurements on ITO/alkali halide/polymer/Ba/Al diodes support injection of holes at bias voltages close to the bandgap of the alkali halide.¹⁴ Moreover, for pristine diodes, the onset of electroluminescence coincides with electroforming.¹⁵ The injected hole can recombine with an electron forming an exciton. Electroluminescence from ITO/CsI/Al diodes confirms injection and recombination of electrons and holes in the alkali halide.¹⁴

Excitons in alkali halides are known to undergo self-trapping, a process involving displacement of a halide atom away from its equilibrium position (Fig. 5(d)). At ambient temperature, the self-trapped exciton can dissociate into a Frenkel defect pair consisting of an anion vacancy filled with an electron (*F*-center) and a halide interstitial (*H*-center, Fig. 5(e)).^{11,16,20,21} Under prolonged bias stress, defects will accumulate and *F*-center aggregates are formed, similar to the case of optical defect generation in LiF by short laser pulses (Fig. 5(f)).²²

Electronic transitions between quantized states of the confined electron associated with the *F* centers give rise to intense defect absorption bands and strong coloration. Due to the more extended delocalization of the electrons in the aggregated defects, the optical transitions in aggregated defects occur at lower photon energies in comparison with isolated defects. The prominent defect absorption band at 1 eV for CsI illustrated in Fig. 3 is consistent with the *M* band attributed to two neutral *F* centers on adjacent lattice positions.²³ Similarly, the defect band at 1.5 eV in LiF can also be assigned to aggregated *F*-centers, viz., F_2^+ and F_4 defects.²⁴ We note that in the spectral region where the neutral polymer has its lowest allowed absorption band (3.0–3.5 eV), a signal with sigmoidal bandshape is observed that matches the electro-absorption spectrum of the neutral polymer.²⁵ No significant bleaching of ground state absorption is observed, indicating that the density of charge carriers residing on the polymer is small.

When the *F*-centers or its aggregates lose an electron, the vacancies acquire a net positive charge relative to the perfect lattice. Similarly, when *H*-centers capture an electron, they become negatively charged (H^-). Under the influence of the applied bias, defects can migrate,^{26,27} and here, we assume that the ionized *F*-centers (F^+) migrate to the alkali halide/polymer interface, while H^- defects move to the ITO/alkali halide contact.

The well-established mobility of charged defects in alkali halides provides an explanation for the apparently very low injection barrier for holes. Accumulation of negatively charged interstitials at the ITO contact lowers the barrier for hole injection (Fig. 5(h)). The hole current increases, more charged defects are formed which results in further lowering of the injection barrier. This self-accelerating process mitigates the restriction of injection barriers on the charge injection. With the restrictions on injection removed, exciton generation is effectively limited by energy conservation and sets in for voltages exceeding the bandgap of the alkali halide. Consequently, the electrocoloration voltage is thickness independent and related to the bandgap of the alkali halide.

In summary, the electrocoloration provides direct experimental evidence for voltage induced defect formation in alkali halides. The correlation between electrocoloration voltage, electroforming voltage, and bandgap of the alkali halides indicates that electroforming occurs when the defect density exceeds $10^{25}/\text{m}^3$, based on the areal density of 4×10^{17} charges/ m^2 just prior to electroforming and the layer thickness. The density for electroforming is close to the critical defect density for the insulator-to-metal transition from the Mott criterion²⁸ ($N_{\text{crit}} \cong (1/5 a_{\text{H}})^3 = 7 \times 10^{25}/\text{m}^3$; a_{H} the Bohr radius in the alkali halide with $\epsilon_r = 9$), suggesting that the electroformed alkali halide layer behaves as a highly doped semiconductor with metallic transport characteristics. The voltage-driven electrocoloration in the alkali halide diodes under study here resembles the behavior of organic semiconductors with combined ionic and electrical conductivity in light emitting electrochemical cells. Application of bias voltage exceeding the bandgap of the semiconductor results in bipolar charge carrier injection via electrochemically doped interface regions near the contacts, independent of the work function of the electrodes used.²⁹

The work forms part of the research programme of the Dutch Polymer Institute (DPI), Project DPI #704, BISTABLE. We gratefully acknowledge the financial support received from Fundação para Ciência e Tecnologia (FCT) through the research Instituto de Tele-comunicações (IT-Lx), the Project Memristor based Adaptive Neuronal Networks (MemBrAiNN), PTDC/CTM-NAN/122868/2010, and funding from the European Commission Seventh Framework Programme FP7/2007-2013' project 212311, ONE-P and from the Dutch Ministry of Education, Culture and Science (Gravity Program 024.001.035).

¹J. Hutchby and M. Garner, *Assessment of the Potential & Maturity of Selected Emerging Research Memory Technologies Workshop & ERD/ERM Working Group Meeting (April 6-7, 2010)* (ITRS Edition, 2010), available at http://www.itrs.net/Links/2010ITRS/2010Update/ToPost/ERD_ERM_2010FINALReportMemoryAssessment_ITRS.pdf.

²G. Deamaley, A. M. Stoneham, and D. V. Morgan, *Rep. Prog. Phys.* **33**, 1129 (1970).

³D. P. Oxley, *Electrocomponent Sci. Technol.* **3**, 217 (1977).

⁴H. Pagnia and N. Sotnik, *Phys. Status Solidi* **108**, 11 (1988).

⁵F. Pan, S. Gao, C. Chen, C. Song, and F. Zeng, *Mater. Sci. Eng. R* **83**, 1 (2014).

⁶M. Depas, T. Nigam, and M. M. Heyns, *IEEE Trans. Electron Devices* **43**, 1499 (1996).

⁷M. D. Pickett and R. S. Williams, *Nanotechnology* **23**, 215202 (2012).

⁸S. Tappertzhofen, I. Valov, and R. Waser, *Nanotechnology* **23**, 145703 (2012).

⁹P. J. Kuekes, N. J. Quitoriano, and J. Yang, *Int. Pat. Appl. WO2010085225-A1*.

¹⁰F. Verbakel, S. C. J. Meskers, R. A. J. Janssen, H. L. Gomes, M. Cölle, M. Büchel, and D. M. de Leeuw, *Appl. Phys. Lett.* **91**, 192103 (2007).

¹¹W. B. Fowler, *The Physics of Color Centers* (Academic Press, 1968).

¹²R. T. Williams and K. S. Song, *J. Phys. Chem. Solids* **51**, 679 (1990).

¹³B. F. Bory, S. C. J. Meskers, R. A. J. Janssen, H. L. Gomes, and D. M. de Leeuw, *Appl. Phys. Lett.* **97**, 222106 (2010).

¹⁴See supplementary material at <http://dx.doi.org/10.1063/1.4903831> for electroforming and electrocoloration data.

¹⁵B. F. Bory, H. L. Gomes, R. A. J. Janssen, D. M. de Leeuw, and S. C. J. Meskers, *J. Phys. Chem. C* **116**, 12443 (2012).

¹⁶K. S. Song and R. T. Williams, *Self Trapped Excitons*, 2nd ed. (Springer Verlag, 1996).

¹⁷H. T. Nicolai, A. Hof, J. L. M. Oosthoek, and P. W. M. Blom, *Adv. Funct. Mater.* **21**, 1505 (2011).

¹⁸C. H. Seager and D. Emin, *Phys. Rev. B* **2**, 3421 (1970).

- ¹⁹B. F. Bory, Ph.D. thesis, Eindhoven University of Technology, 2014.
- ²⁰H. N. Hersh, *Phys. Rev.* **148**, 928 (1966).
- ²¹P. H. Bunton, R. F. Haglund, Jr., D. Liu, and N. H. Tolk, *Phys. Rev. B* **45**, 4566 (1992).
- ²²I. Chiamenti, F. Bonfigli, A. S. L. Gomes, F. Michelotti, R. M. Montecali, and H. J. Kalinowski, *J. Appl. Phys.* **115**, 023108 (2014).
- ²³D. B. Sirdeshmukh, L. Sirdeshmukh, and K. G. Subhadra, *Alkali Halides: A Handbook of Physical Properties* (Springer Verlag, 2001).
- ²⁴G. Baldacchini, *J. Lumin.* **100**, 333 (2002).
- ²⁵M. Tong, C. X. Sheng, and Z. V. Vardeny, *Phys. Rev. B* **75**, 125207 (2007).
- ²⁶G. M. Loubriel, T. A. Green, P. M. Richards, R. G. Albridge, D. W. Cherry, R. K. Cole, R. F. Haglund, Jr., L. T. Hudson, M. H. Mendenhall, D. M. News, P. M. Savundararaj, K. J. Snowdon, and N. H. Tolk, *Phys. Rev. Lett.* **57**, 1781 (1986).
- ²⁷N. A. Seifert, H. Ye, D. Liu, R. G. Albridge, A. V. Barnes, N. Tolk, W. Husinsky, and G. Betz, *Nucl. Instrum. Methods Phys. Res. B* **72**, 401 (1992).
- ²⁸N. F. Mott, *Metal-Insulator Transitions*, 2nd ed. (Taylor and Francis, 1990).
- ²⁹Q. Pei, G. Yu, C. Zhang, Y. Yang, and A. J. Heeger, *Science* **269**, 1086 (1995).